F. FORGHANY[1], A. ASDOLLAHI-GHOHIEH[2], M. TAIEBI-RAHNI[3]

1 - Science and Research Branch, Islamic Azad University, Tehran, Iran
2 - Civil Aviation Technology College, Tehran, Iran
3 - Sharif University of Technology, Tehran, Iran

NUMERICAL INVESTIGATION OF THE FLUIDIC INJECTION ANGLE EFFECTS ON THRUST VECTORING

A computational investigation of the fluidic injection angle effects on fluidic thrust vectoring was conducted. Simulation of a two-dimensional convergent-divergent (2DCD) nozzle with shock-vector control method of fluidic injection for pitch vector control was performed with the computational fluid dynamics, using Spalart-Allmaras (S-A) one equation turbulence model. Nozzle design included fluidic variables and injection angle. The secondary flow was injected through a slot in the upper divergent wall. A nozzle pressure ratio (NPR) of 4.6.was assumed. Variable secondary pressure ratios (SPR) from 0.7 to 1.6 were investigated at M∞=0.05; which correspondeds to secondary mass flow rates of 4% to 10% of the primary mass flow rate. The effect of variable fluidic injection angle from 60° to 120° on pitch thrust vector angle and thrust vectoring efficiency were investigated. Computational results indicates that increasing SPR in all cases, increased pitch thrust vector angle and decreased thrust vectoring efficiency; also the greatest pitch thrust vector angle was achieved in the smaller fluidic injection angle.

Key words: *Thrust Vectoring, Shock Vector Control, Optimize Fluidic Injection Angle.*

Introduction

Thrust vectoring is a candidate technology for the next generation aircrafts that may help satisfy take-off and landing requirements. Additionally, thrust vectoring could augment conventional controls for some control power to trim the aircraft and thus reduce cruise trim drag. Thrust vectoring can be a valuable control effector at low dynamic pressures, where traditional aerodynamic control technologies are less effective. There are two fundamental methods to accomplish thrust vectoring, namely mechanical and fluidic. Fluidic thrust vectoring offers the potential for structurally fixed nozzles, which have the potential for substantial weight reductions compared to mechanical thrust vectoring nozzles that require actuated hardware to force the exhaust flow off axis. Fluidic thrust vectoring is the control of the primary exhaust flow with use of a secondary air source, which typically bleeds air from the engine compressor or fan. Three primary mechanisms of fluidic thrust vectoring that have been studied over the last 15 years are: shock-vector control, throat shifting, and counterflow. These techniques can be used to vector the exhaust flow in the pitch and yaw directions. All thrust vectoring techniques are evaluated with some common parameters such as: thrust vector angle and thrust vectoring efficiency. Thrust vectoring efficiency () is an important parameter to evaluate and compare the ability of different configurations to vector the primary exhaust flow with a given amount of secondary fluidic injection [1-14].

The shock-vector control (SVC) method [2-9] uses supersonic flow turning through shocks created by fluidic injection in the divergent section of a convergent-divergent (CD) nozzle. Working best at off-design, over-expanded flow conditions, large thrust vector angles are generated with SVC techniques in expense of system thrust ratio as the flow is robustly turned and losses occur through shocks in the nozzle. Throat shifting (TS) methods [9-12] manipulate the subsonic flow upstream of the throat more efficiently. This technique shifts and skews the nozzle throat plane by fluidic injection in nozzle throat and typically achieves higher system thrust ratios than shock-vector control methods, but usually generates smaller thrust vector angles. Unlike the two previously described thrust-vectoring techniques, the counterflow method uses suction in a slot between a primary CD nozzle and an aft collar [13-14]. The counterflow technique can produce large thrust vector angles with little secondary suction flow requirements, but issues hysteresis effects such as suction supply source and airframe integration. The current investigation attempted to initiate a database of secondary flow injection angle effects on fluidic thrust vectoring. The nozzle under investigation was a two-dimensional, convergent-divergent (2DCD) rectangular nozzle with fluidic injection for pitch thrust vector control. The secondary air stream was injected through a slot in the upper divergent wall. Simulations were computed with nozzle pressure ratio (NPR) of 4.6, secondary pressure

ratios (SPR) from 0.7 to 1.6 and with M∞=0.05 to document the effect of the fluidic injection angle on vectoring effectiveness and thrust vectoring efficiency (corresponding to secondary mass flow rates of 4% to 10% of the primary mass flow rate, respectively) [15-17]. In addition, a comparison between computational and experimental results [15] was made to validate our computational method as a viable tool for predicting nozzle flows with injection streams. This study was meant to produce optimal configurations of secondary flow injection angle for fluidic thrust.

1. Computational Method

The CFD code PMB3D (Parallel Multi-Block, three-dimensional) was developed and used to predict thrust vectoring efficiency, internal nozzle performance, and fluidic thrust vectoring by convergent-divergent rectangular nozzle concept. PMB3D requires a structured-mesh computational domain and a multi-block feature to allow the domain to be partitioned into different sections, which is critical for modeling complex configurations (like the 2DCD and for efficiently, running the parallel version). Our Explicit, finite-volume flow solver represents the three-dimensional (3D), unsteady Reynolds-averaged Navier-Stokes (URANS) equations. The URANS equations were solved together with the Spalart-Allmaras (S-A) one equation turbulence model for closure of the URANS equations. AUSM+ flux splitting scheme and 4th order Runge-Kutta scheme for time integration were all implemented in each block. MUSCL interpolation was used to provide high order accuracy with the Van Albada limiter to prevent spurious oscillations across shock waves [18-25].

A first order extrapolation outflow condition was used at downstream far field boundary. The stagnation conditions were specified in nozzle inlet and the injection port with total pressure boundary condition and a fixed total temperature. A no-slip adiabatic wall boundary conditions was implemented on nozzle surfaces to obtain viscous solutions.

The nozzle used in this study was an axisymmetric, rectangular, two-dimensional CD nozzle from NASA Langley Research Center [15]. The length of the nozzle was 115.57 mm, while the nozzle width was 101.346 mm. In addition, the throat area of the nozzle was 2785.19 mm^2, half height of the throat was 13.741 mm, and 57.785 mm from throat to inlet. The area ratio of the nozzle outlet to the throat (expansion ratio) was 1.796 and nozzle divergence angle was 11.01°. The nozzle inlet center was set to be the origin of coordinates, the secondary inlet located at 104.14 mm and the length of slot was 2.032 mm (Fig's. 1-2).

The computational mesh was three-dimensional with 8 blocks defining the internal nozzle, 1 block representing the injection plenum, and 10 blocks representing the external freestream domain. The injection plenum (Fig. 3) had one-to-one grid matching with the nozzle divergent section mesh. The far field was located 2 nozzle lengths upstream and 8 nozzle lengths downstream of the nozzle exit. The upper and lower lateral far field was located 6 body lengths above and below the nozzle. The first grid height in the boundary layer was defined for y+<1.5 on the fine mesh spacing for adequate modeling of the boundary layer flow and its interaction with secondary flow injection.

2. Results

A computational investigation of the aerodynamic effects on fluidic thrust vectoring has been conducted. Simulation of a two-dimensional, convergent-divergent (2DCD) nozzle with shock-vector control method of fluidic injection for pitch vector control were performed using URANS approach and Spalart-Allmaras one equation turbulence model. Nozzle design included a variable fluidic injection angle. Simulations were conducted for nozzle pressure ratio (NPR) of 4.6 and variable secondary pressure ratios (SPR) from 0.7 to 1.6 and with M∞=0.05, corresponding to secondary mass flow rates of 4% to 10% of the primary mass flow rate. The effect of variable fluidic injection angle (from 60° to 120°) on pitch thrust vector angle and thrust vectoring efficiency were investigated (Fig. 4). The performance of fluidic thrust vectoring (FTV) was evaluated by thrust vector angle and thrust vectoring efficiency in the nozzle exit. The effect of fluidic thrust vectoring parameters, such as NPR, SPR, and fluidic injection angle on FTV performance were studied.

2.1. Code Validation

Our computational results were compared with experimental data of Ref. [15]. The centerline pressure at, SPR=0.7 (4% of primary mass flow rate) is shown in Fig. 1. Our PMB3D results for pitch thrust vector angle and static pressures along the upper and lower nozzle surfaces correlated well with experimental data (with a few correlate well with experimental data (with a few notable exceptional points near shock). The shock location, at the upper surface was predicted to be x/xt=1.56 (xt is axial location of throat), while it was 1.53 in the experiment. Our results at the lower surface gave x/xt=1.91, compared to 1.89 found by the above experimental (Fig. 5).

2.2. Effect of SPR

In all cases, increasing SPR, increases pitch thrust vector angle and decreases thrust vectoring

efficiency. The effect of the oblique shock or oblique expansion waves becomes strong by increasing the mass flow rate of the fluidic injection (increasing 2% of mass flow rate per increasing 0.3 of SPR). Increasing secondary injection flow rate decreases the effective minimum area in the nozzle, which substantially decreases thrust vectoring efficiency by total pressure losses due to shocks and separated flow. Fig. 6, shows the Mach number shadowgraph along the nozzle for NPR=4.6 and variable SPR. As shown in this figure, the thrust vector angle increases with percent injection, although the thrust vectoring efficiency is much higher in lower injection rates. Pressure distribution along the nozzle, NPR=4.6, SPR=0.7 (4% of primary mass flow rate), are shown in Fig. 7. Similar trends are witnessed for SPR=1.0 (6% of primary mass flow rate), SPR=1.3 (8% of primary mass flow rate), and SPR=1.6 (10% of primary mass flow rate). Increasing SPR increases the strength of the oblique shock and moves the shock upstream, as shown in upper surface (Fig. 8). The pressure distributions by increasing SPR shown in Fig. 8 helps to explain improvement to pitch thrust vector angle. The shock and flow separation from the upper wall moves

further upstream, then, reattaches the upper wall near, as injection total pressure increases.

The effect of increasing total pressure of the secondary injection stream has positive impact on thrust vector angle and negative impact on thrust vectoring efficiency. The increased pressure differential along the upper and lower wall, results in improved pitch vector angle. Finally, the effect of increasing total pressure of the secondary injection stream has positive impact on thrust vector angle and negative impact on thrust vectoring efficiency.

2.3. Effect of Fluidic Injection Angle

The highest thrust vector angle in variable SPR (which is achieved from 10.32° to 19.27° by the fluidic injection angles) was varied from 110° to 85° with improvement from 36.3% to 8.31%. In addition, the greatest pitch thrust vector angle with increasing SPR is achieved in the smaller fluidic injection angle. The best thrust vectoring efficiency, which was achieved from 3.446°/%- injection to 1.958°/%-injection by the fluidic injection angles is varied from 120° to 85° with improvement from 44.1% to 9.03%, (Table 1 & Fig. 9).

Table 1

Effect of fluidic injection angles on internal performance improvement

Case 1			Fluidic injection angle (optimize)			Fluidic injection angle (normal to boundary)			Improvement	
NPR	M∞	SPR	φ (deg)	δ_p (deg)	η (deg/%inj)	φ (deg)	δ_p (deg)	η (deg/%inj)	δ_p %	η %
4.6	0.05	0.7	110	10.329	3.099	78.99	7.578	2.151	36.3	44.1
		1	110	14.274	2.925	78.99	11.167	1.965	27.8	48.8
		1.3	100	17.626	2.555	78.99	14.391	1.961	22.4	30.2
		1.6	85	19.279	2.135	78.99	17.799	1.958	8.31	9.03
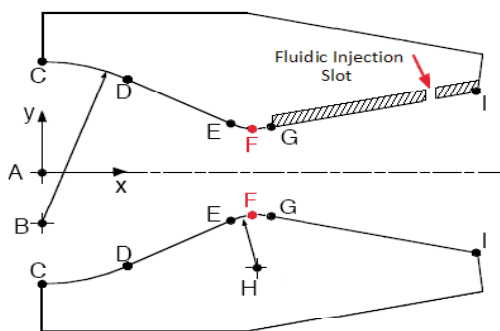
Point	Coordinat	
	X, mm	Y, mm
A	0	0
B	0	-15.595
C	0	35.204
D	23.291	29.541
E	50.495	15.519
F	57.785	13.741
G	60.807	14.046
H	57.785	29.616
I	115.57	24.688

All positions measured from centerline of nozzle

Fig. 1. Sketch of the geometric design for 2DCD rectangular fluidic thrust vectoring nozzle (x-y plane)
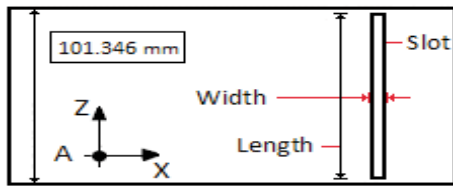
X, mm	Length, mm	Width, mm
104.14	88.646	2.032

Fig. 2. Sketch of the design injection slot for 2DCD rectangular fluidic thrust vectoring nozzle (x-z plane)
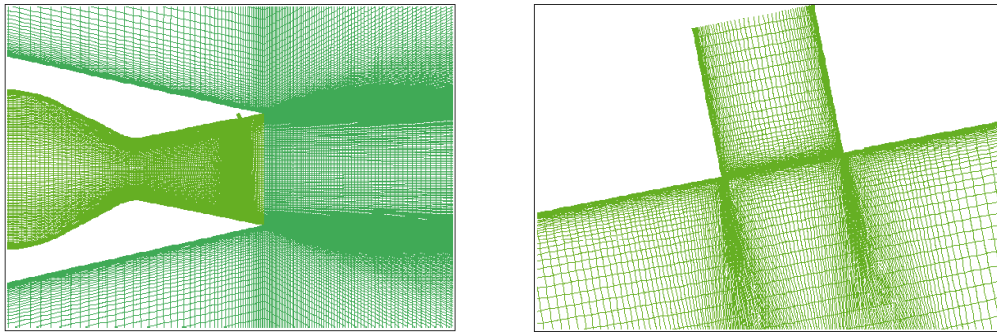
Fig. 3. The computational domain representing the 2DCD nozzle with ainjection plenum (the injecton plenum has one-to-one grid matching with the primary nozzle grid)
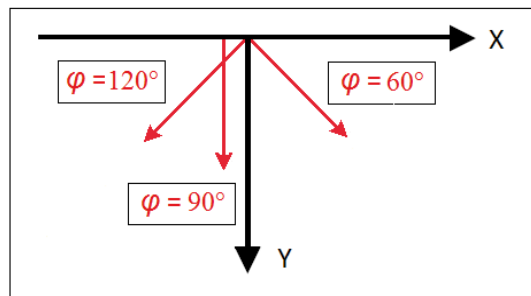
Fig. 4. Diagram of fluidic injecton angle in two-dimensions (x-y plane)
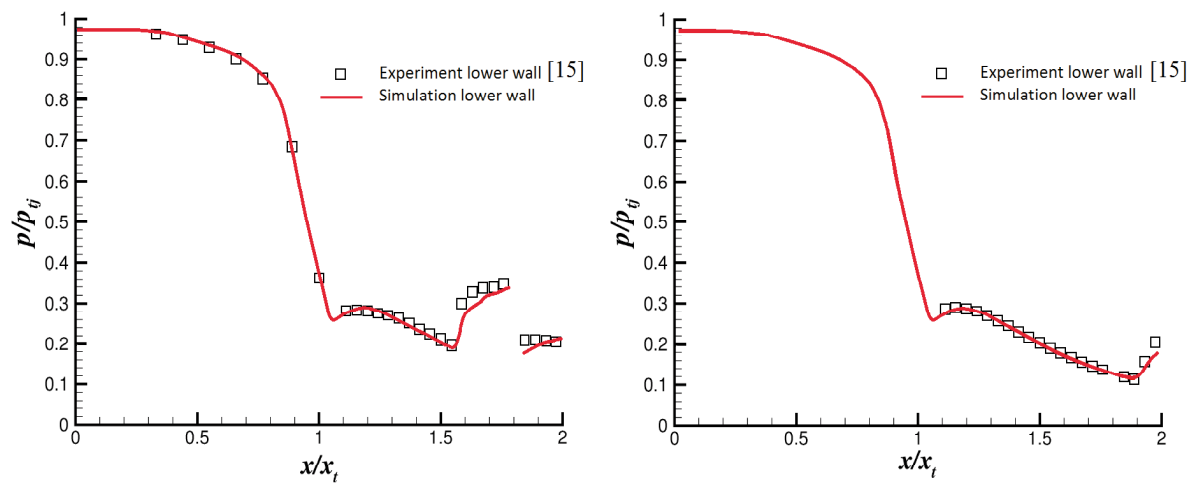
Fig. 5. Experimental and comptational centerline pressures along internal nozzle upper wall, NPR=4.6, SPR=0.7, static freestream conditions
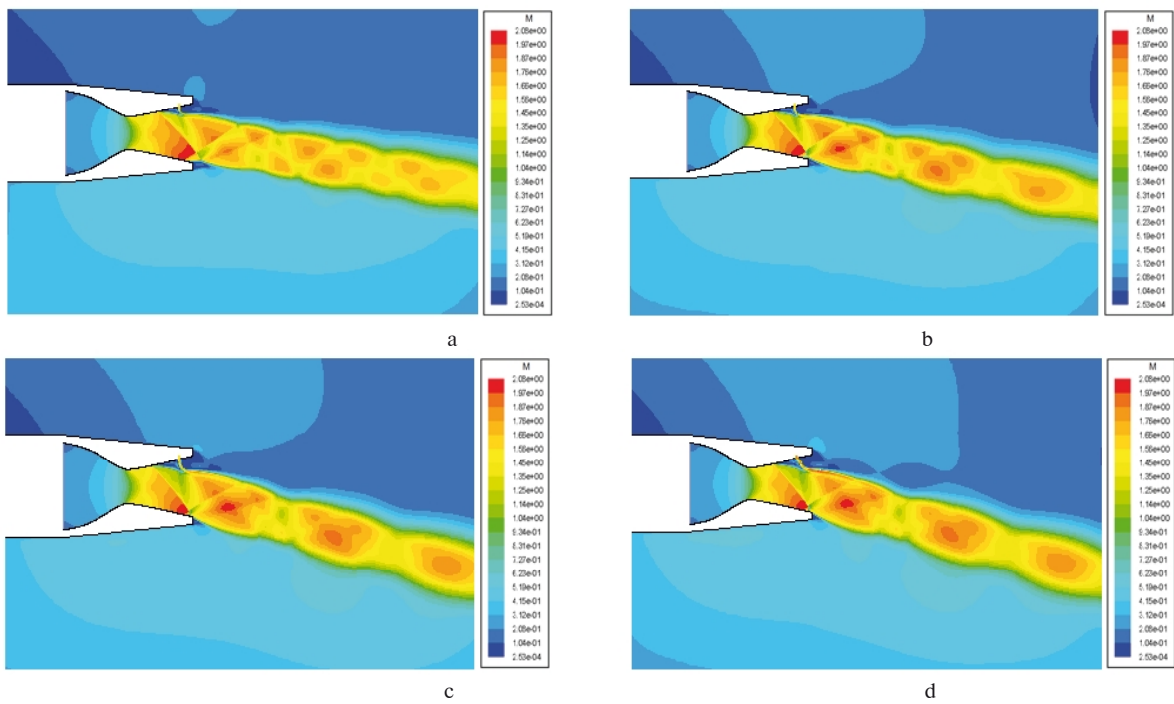
Fig. 6. Mach number shadowgraph inside and outside the nozzle at NPR=4.6 and (a) SPR=0.7, (b) SPR=1.0, (c) SPR=1.3, (d) SPR=1.6
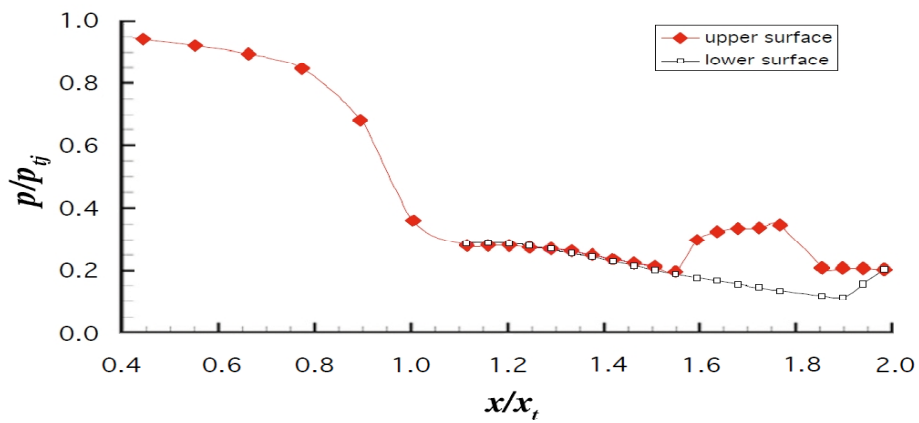
Fig. 7. Pressure distribution along the nozzle at NPR = 4.6 and SPR = 0.7
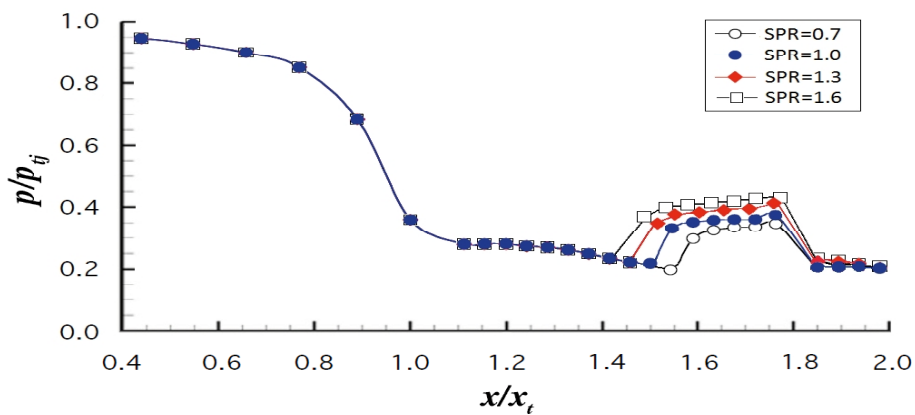
Fig. 8. Pressure distribution of upper surface along the nozzle at NPR = 4.6
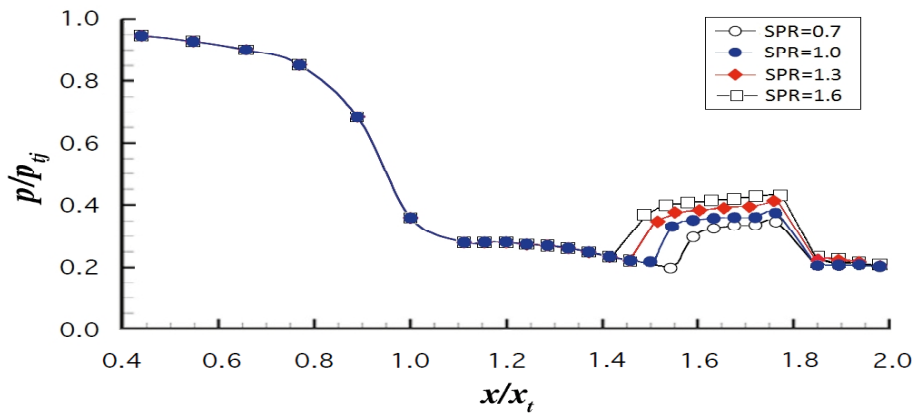
Fig. 8. Pressure distribution of upper surface along the nozzle at NPR = 4.6
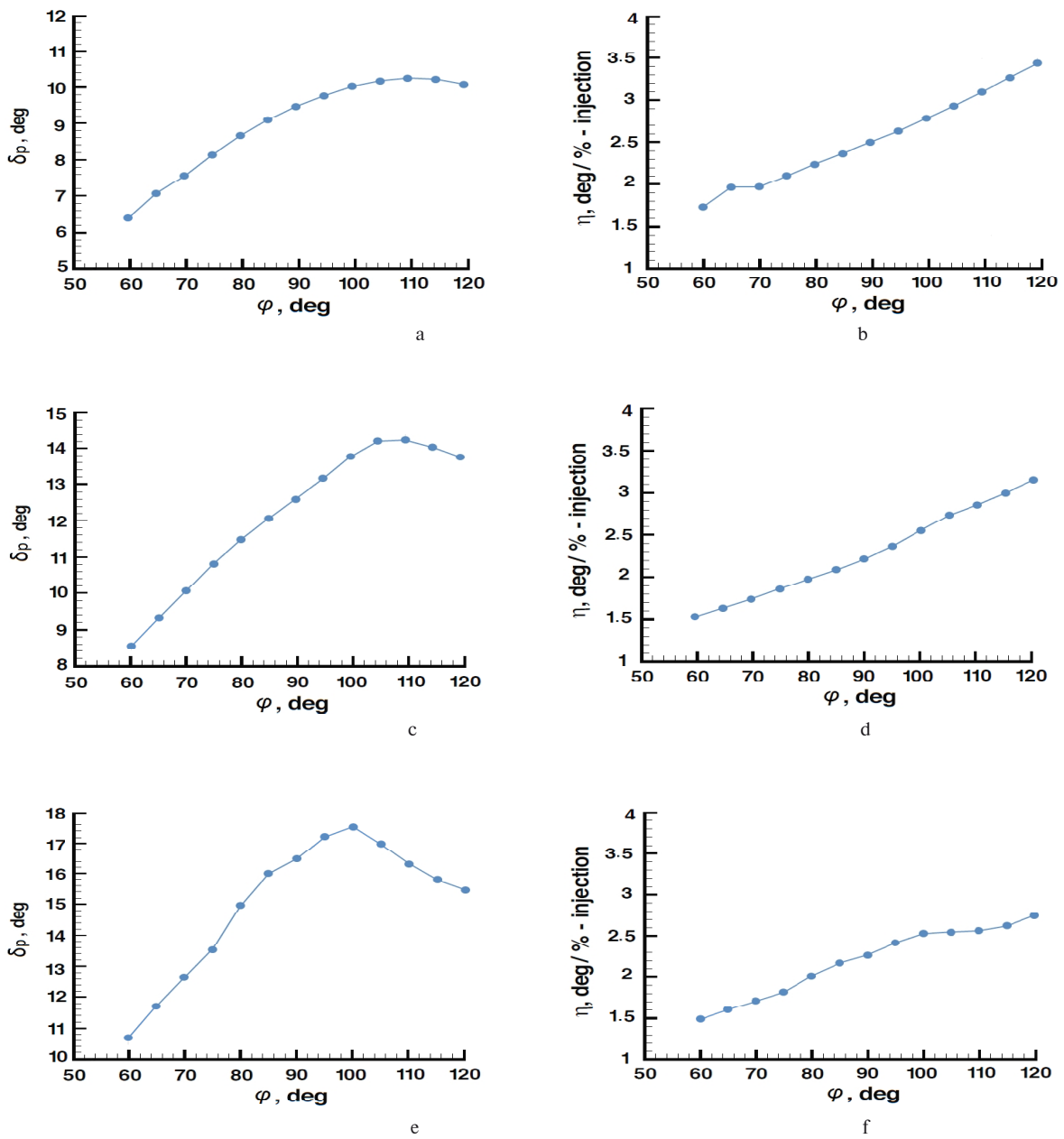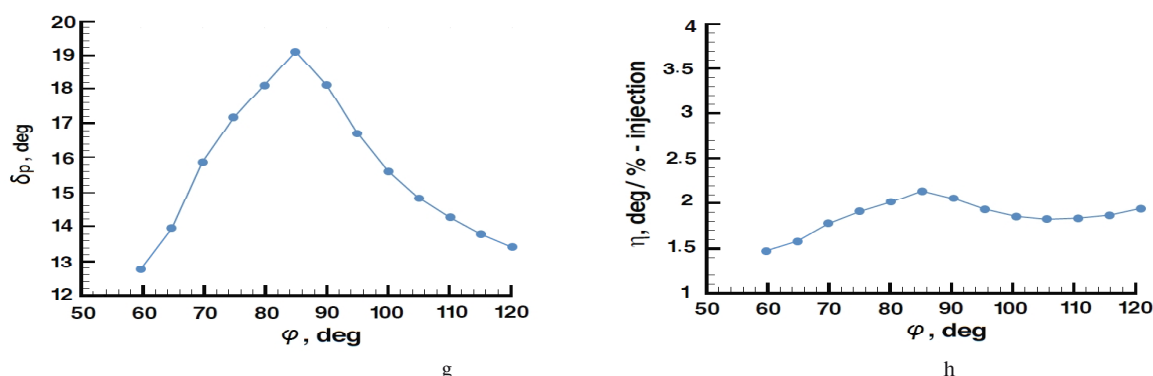
Fig. 9. Pitch thrust vector angle and thrust vectoring efficiency at NPR=4.6 and (a)(b) SPR=0.7, (c)(d) SPR=1.0, (e)(f) SPR=1.3 and (g)(h) SPR=1.6

Conclusion

A computational investigation of the aerodynamic effects on fluidic thrust vectoring has been conducted. The effect of variable fluidic injection angle (from 60° to 120°) on pitch thrust vector angle and on thrust vectoring efficiency were investigated. The performance of fluidic thrust vectoring (FTV) was evaluated by studying thrust vector angle and thrust vectoring efficiency in nozzle exit. The effects of fluidic thrust vectoring parameters, such as NPR, SPR, and fluidic injection angle on FTV performance were studied. The data from the current computational investigation indicate that:

1. In all cases, increasing SPR, increases pitch thrust vector angle and decreases thrust vectoring efficiency (the effect of the oblique shock or oblique expansion waves become strong by increasing the mass flow rate of the fluidic injection; increasing 2% of mass flow rate per increasing 0.3 of SPR). Increasing secondary injection flow rate decreases the effective minimum area in the nozzle, which substantially increased pitch thrust vector angle and decreases thrust vectoring efficiency. The effect of increasing total pressure of the secondary injection stream has positive impact on thrust vector angle and negative impact on thrust vectoring efficiency,

2. The highest thrust vector angle in variable SPR (which is achieved from 10.32° to 19.27° by the fluidic injection angles) is varied from 110° to 85° with improvement from 36.3% to 8.31%. Also, the greatest pitch thrust vector angle with increasing SPR is achieved in the smaller fluidic injection angle, and

3. The best thrust vectoring efficiency is achieved from 3.446°/%- injection to 2.135°/%-injection by the fluidic injection angles varied from 120° to 85° with improvement from 44.1% to 9.03%.

References

1. Deere K.A., Flamm J.D., Berrier B.L., and Johnson, S.K.: Computational Study of an Axisymmetric Dual Throat Fluidic Thrust Vectoring Nozzle for a Supersonic Aircraft Application, AIAA-2007-5085, July 2007.

2. Anderson C.J., Giuliano V.J., and Wing, D.J.: Investigation of Hybrid Fluidic / Mechanical Thrust Vectoring for Fixed-Exit Exhaust Nozzles. AIAA 97-3148, July 1997.

3. Abeyounis W.K., and Bennett B.D.: Static Internal Performance of an Overexpanded, Fixed-Geometry, Nonaxisymmetric Nozzle with Fluidic Pitch-Thrust-Vectoring Capability, NASA TP-3645, October 1997.

4. Chiarelli C., Johnsen R. K., Shieh C. F., Wing D.J.: Fluidic Scale Model Multi-Plane Thrust Vector Control Test Results, AIAA Paper 93-2433, June 1993.

5. Giuliano V.J., and Wing D.J.: Static Investigation of a Fixed-Aperture Exhaust Nozzle Employing Fluidic Injection for Multiaxis Thrust Vector Control, AIAA Paper 97-3149, July 1997.

6. Wing D.J.; and Giuliano V.J.: Fluidic Thrust Vectoring of an Axisymmetric Exhaust Nozzle at Static Conditions, ASME FEDSM97-3228, June 1997.

7. Deere K. A.: Computational Investigation of the Aerodynamic Effects on Fluidic Thrust Vectoring, AIAA-2000-3598, July 2000.

8. Waithe K.A.: An Experimental and Computational Investigation of Multiple Injection Ports in a Convergent-Divergent Nozzle for Fluidic Thrust Vectoring, Master of Science Thesis, May 2001.

9. Deere K.A.: Summary of Fluidic Thrust Vectoring Research Conducted at NASA Langley Research Center, AIAA-2003-3800, June 2003.

10. Yagle P.J., Miller D.N., Ginn K.B.; and Hamstra J.W.: Demonstration of Fluidic Throat Skewing for Thrust Vectoring in Structurally Fixed Nozzles, 2000-GT-0013, May 8-11, 2000.

11. Deere K.A.; and Wing D.J.: PAB3D Simulations of a Nozzle with Fluidic Injection for Yaw-Thrust-Vector Control, AIAA Paper 98-3254, July 1998.

12. Miller D.N.; Yagle P.J.; and Hamstra J.W.: Fluidic Throat Skewing for Thrust Vectoring in Fixed Geometry Nozzles, AIAA Paper 99-0365, January 1999.

13. Hunter C.A. and Deere K.A.: Computational Investigation of Fluidic Counterflow Thrust Vectoring, AIAA Paper 99-2669, June 1999.

14. Flamm J.D.: Experimental Study of a Nozzle Using Fluidic Counterflow for Thrust Vectoring, AIAA Paper 98-3255, July 1998.

15. Waithe K.A. and Deere K.A.: Experimental and Computational Investigation of Multiple Injection Ports in a Convergent-divergent Nozzle for Fluidic Thrust Vectoring, the 21st AIAA Applied Aerodynamics Conference, AIAA-2003-3802.

16. Deere K.A.: Propulsion simulations with the unstructured-grid CFD tool TetrUSS, AIAA 2002-2980.

17. Deere K.A.: Computational Investigation of the Aerodynamic Effects on Fluidic Thrust Vectoring, AIAA-2000-3598, July 2000.

18. Spalart P.; and Allmaras S.A.: One-equation turbulence model for aerodynamic flows, AIAA Paper 92-0439, January 1992.

19. Liou M.S.: Ten Years in the Making AUSA-family, AIAA Paper 2001-2521, Jun. 2001.

20. Liou M.S.: A Continuing Search for a Near-Perfect Numerical Flux Scheme, Technical Memorandum 106524, NASA, Mar. 1994.

21. Liou M.S.: A New Flux Splitting Scheme. Journal of Computational Physics, Vol. 107, pp. 23-39, 1993.

22. Muller B.; and Rizzi A.: Runge-Kutta Finite Volume Simulation of Laminar Transonic Flow over a NACA0012 Airfoil, Using the Navier-Stokes Equation, FFA TN 1986-60, 1989.

23. Van Leer B.: Towards the Ultimate Conservative Difference Scheme, Second-Order Sequel to Godunov's Method, Journal of Computational Physics, Vol. 32, No. 1, pp. 101-136, Jul. 1979.

24. Hirsch C.: Numerical Computational of Internal and External Flows, Vol. 2, John Wiley and Sons, Chichester, 1988.

25. Van Albada G.D.; Van Leer B.; and Roberts W.W.: A Comparative Study of Computational Methods in Cosmic Gas Dynamics. Astronomy an Astrophysics, Vol. 108, No. 1, pp. 76-84, 1982.

F. Forghany, A. Asdollahi-Ghohieh, M. Taiebi-Rahni. Чисельні дослідження впливу кута вдуву струменя на відхилення вектора тяги

Проведено чисельні дослідження впливу кута вдуву вторинного струменя на відхилення вектора тяги. Моделювання двовимірного сопла зі звуженням-розширенням було виконано з використанням методу контролю стрибка ущільнення і керування вдувом струменя для керування вектором тангажа із застосуванням методів обчислювальної газодинаміки і з використанням однопараметричної моделі турбулентності Спаларта-Аллмараса. Розрахункові параметри сопла в якості змінних включали параметри потоку і кут вдуву вторинного струменя. Вдув вторинного потоку здійснювався через вузький отвір у верхній стінці, що розширюється. Прийнято ступінь підвищення тиску газу в соплі рівною 4,6. Ступінь підвищення тиску вторинного потоку, що змінюється, у межах 0,7 - 1,6 досліджувалася при $M\infty = 0{,}05$, що відповідає масовій витраті вторинного потоку рівному від 4 до 10% масової витрати первинного потоку. Проведено дослідження впливу кута вдуву струменя, змінюваного від 60 до 120°, на векторний кут тангажа і ккд вектора тяги, що відхиляє. Результати розрахунків показують, що у всіх випадках збільшений ступінь підвищення тиску вторинного потоку приводить до збільшення кута вектора тяги, що відхиляється, і ккд вектора тяги, що відхиляється, а також максимальний кут вектора тяги, що відхиляється, було отримано при меншому куті вдуву струменя.

Ключові слова: відхилення вектора тяги, контроль напрямку стрибка, оптимізація кута вдуву струменя.

F. Forghany, A. Asdollahi-Ghohieh, M. Taiebi-Rahni. Численные исследования влияния угла вдува струи на отклонение вектора тяги

Проведены численные исследования влияния угла вдува вторичной струи на отклонение вектора тяги. Моделирование двумерного сопла с сужением-расширением было выполнено с использованием метода контроля скачка уплотнения и управления вдувом струи для управления вектором тангажа с применением методов вычислительной газодинамики и с использованием однопараметрической модели турбулентности Спаларта-Аллмараса. Расчетные параметры сопла в качестве переменных включали параметры потока и угол вдува вторичной струи. Вдув вторичного потока осуществлялся через узкое отверстие в верхней расширяющейся стенке. Принята степень повышения давления газа в сопле равная 4,6. Степень повышения давления изменяющегося вторичного потока в пределах 0,7 — 1,6 исследовалась при $M\infty = 0{,}05$, что соответствует массовому расходу вторичного потока равному от 4 до 10% массового расхода первичного потока. Проведено исследование влияния угла вдува струи, изменяемого от 60 до 120°, на векторный угол тангажа и кпд отклоняемого вектора тяги. Результаты расчетов показывают, что во всех случаях увеличенная степень повышения давления вторичного потока приводит к увеличению угла отклоняемого вектора тяги и кпд отклоняемого вектора тяги, а также максимальный угол отклоняемого вектора тяги были получены при меньшем угле вдува струи.

Ключевые слова: отклонение вектора тяги, контроль направления скачка, оптимизация угла вдува струи.